Electronic structure and bonding properties of Si-doped hydrogenated amorphous carbon films

S. C. Ray, C. W. Bao, H. M. Tsai, J. W. Chiou, J. C. Jan, K. P. Krishna Kumar, and W. F. Pong[a)]
Department of Physics, Tamkang University, Tamsui, Taiwan 251, Republic of China

M.-H. Tsai
Department of Physics, National Sun Yat-Sen University, Kaohsiung, Taiwan 804, Republic of China

W.-J. Wang and C.-J. Hsu
Department of Chemistry, Tamkang University, Tamsui, Taiwan 251, Republic of China

T. I. T. Okpalugo, P. Papakonstantinou, and J. A. McLaughlin
NIBEC, School of Electrical and Mechanical Engineering, University of Ulster, County Antrim BT370QB, Northern Ireland, United Kingdom

(Received 14 May 2004; accepted 2 September 2004)

This work investigates the C *K*-edge x-ray absorption near-edge structure (XANES), valence-band photoelectron spectroscopy (PES), and Fourier transform infrared (FTIR) spectra of Si-doped hydrogenated amorphous carbon films. The C *K*-edge XANES and valence-band PES spectra indicate that the sp^2/sp^3 population ratio decreases as the amount of tetramethylsilane vapor precursor increases during deposition, which suggest that Si doping% enhances sp^3 and reduces sp^2-bonding configurations. FTIR spectra show the formation of a polymeric sp^3 $C-H_n$ structure and $Si-H_n$ bonds, which causes the Young's modulus and hardness of the films to decrease with the increase of the Si content. © *2004 American Institute of Physics*. [DOI: 10.1063/1.1812594]

Diamond-like carbon (DLC) is a unique material useful as a protective overcoating on magnetic disk drives because it has a unique combination of high hardness, low friction and wear, electrical insulation, and chemical inertness.[1] However, several problems have arisen in this usage. DLC as hydrogenated amorphous carbon (*a*-C:H) has limited thermal stability, poor adhesion to some substrates such as steels, high internal stress, and a friction coefficient that strongly depends on the relative humidity of the environment. Si-doped DLC films have been found to stabilize sp^3 bonding, reduce stress and dependence of the friction coefficient on relative humidity, improve adhesion to metal substrates, and increase thermal stability and band gap.[2] A range of hydrogenated amorphous carbon-containing silicon (*a*-C:H:Si) films were deposited on Si(100) substrate by plasma-enhanced chemical vapor deposition (PECVD) method using tetramethylsilane [$Si(CH_3)_4$, TMS] vapor as a Si precursor. Their various structural and mechanical properties were investigated previously.[2] This work focuses on the role and effect of the incorporation of Si on the electronic structure and bonding properties of *a*-C:H:Si thin films.

C *K*-edge x-ray absorption near-edge structure (XANES) and valence-band photoelectron spectroscopy (PES) measurements of *a*-C:H and *a*-C:H:Si films were performed at the National Synchrotron Radiation Research Center (NSRRC), Hsinchu, Taiwan. Fourier transform of the infrared (FTIR) spectra were obtained using the FTIR spectrophotometer for wavelengths in the range between 400 and 3800 cm^{-1}. The films used in this work were prepared by the PECVD method on the Si(100) substrate at a bias voltage of 400 V and at different deposition time. The film compositions, deposition time, thickness, and mechanical properties of these films are presented in Table I and described elsewhere.[2]

Figure 1 displays the normalized C *K*-edge XANES spectra of *a*-C:H and (B_0) and *a*-*C*:H:Si (B_1-B_4) films and the reference graphite. The graphite spectrum shows that π^* and σ^* bands are located at ~285.5 and 291.7 eV, respectively, while the π^* and σ^* bands in the *a*-C:H and *a*-*C*:H:Si spectra are located at ~286.1 and 293.0 eV. The π^* feature is typical of the C=C (sp^2) bond and the σ^* feature is typical of the tetrahedral C–C (sp^3) bond. The 286.1 eV π^* feature in the *a*-C:H and *a*-C:H:Si spectra is higher than that of the C=C bond (~285.5 eV: graphite) but below that of the C–H bond (~288 eV: generally observed in α-C:H film[3,4]) in the XANES spectra of all of the *a*-C:H:Si samples. There is an energy sift of ~0.6 eV. The intensities in all *a*-C:H:Si spectra were also observed to be higher in the range ~288–295 eV but lower in the range ~295–308 eV than those in the *a*-C:H spectrum. This effect can be clearly seen in the difference spectra between *a*-C:H:Si (B_1-B_4) and *a*-C:H (B_0) presented in the inset of Fig. 1. The intensity increases gradually in the region 288–295 eV and decreases slowly in the region 295–308 eV as Si doping increases. This trend can be interpreted as due to the formation of the $C-H_n$ and $Si-H_n$ bonds to be described later in the discussion of the FTIR measurements. None of the prominent Si–C peaks in the XANES spectra, as observed by García *et al.*[5] for diamond nuclei on silicon and Tsai *et al.*[6] for SiC, were observed in this study.

Figure 2 presents the valence-band PES spectra of *a*-C:H and *a*-C:H:Si films obtained using an incident photon energy of 60 eV. The spectrum of the *a*-C:H film is dominated by two overlapping broad peaks centered at around 3 eV (**I**) and 7 eV (**II**), which correspond to p_π and p_σ bands, respectively.[7] The peak positions in the spectra of *a*-C:H:Si films shift gradually from ~3.4 to 4.2 eV for the

a)Author to whom correspondence should be addressed; electronic mail: wfpong@mail.tku.edu.tw

TABLE I. The TMS flow rate, deposition time, film composition, thickness, and Young's modulus of *a*-C:H and *a*-C:H:Si films.

Sample No.	TMS flow	Dep time	Composition (at.%)			Thickness	Young's Modulus
	(sccm)	(s)	C	Si	O	(nm)	*E*(GPa)
a-C:H (B_0)	0	480	84.2	0.30	15.5	178	187.0±0.6
a-C:H:Si (B_1)	05	300	69.4	10.2	20.4	172	156.7±2.3
a-C:H:Si (B_2)	10	180	68.4	18.4	13.2	184	148.5±2.8
a-C:H:Si (B_3)	15	135	62.0	14.5	23.5	166	142.8±3.4
a-C:H:Si (B_4)	20	90	63.2	19.7	17.1	176	141.8±3.4

p_π band and from ~7.2 to 7.9 eV for p_σ band as the TMS flow rate increases. The dominant feature has a shoulder located at 10–11 eV (**III**) and a broad feature at about 17 eV (**IV**) in the spectra of *a*-C:H and *a*-C:H:Si films is also observed. The spectra can be deconvoluted with four Gaussian peaks as shown in inset (a) of Fig. 2 using the spectrum of the B_4 sample as an example. The shift of the dominant feature and the change in intensity can be clearly seen in inset (b) of Fig. 2, in which a common base line (dashed line shown in Fig. 2) was subtracted from all of the spectra. The intensities of peaks **II** and **I** increase and decrease, respectively, as the Si concentration increases, corresponding to the enhancement and reduction of sp^3 and sp^2 states, respectively. This finding implies the formation of sp^3-rich *a*-C:H:Si films with Si incorporation. The shoulder **III** (at ~11 eV) is presumably associated with the C–H_n bonds. Peak **IV** was argued by Reinke *et al.* to be due to the surface plasmon of the sp^2 states.[7]

The FTIR spectra normalized with the thickness shown in Fig. 3 contain absorption peaks of various vibration modes in the 400–3800 cm^{-1} range for the films deposited at different TMS flow rates and the reference Si substrate. The first sharp peak at 612 cm^{-1} and the features in the 700–1000 cm^{-1} range were assigned to the Si–C(*s*) stretching mode[8] and Si–C(*s*), Si–H_n(*s*), and Si–CH_n wagging modes,[9–11] respectively. The peak at 1100 cm^{-1} was assigned to the Si–O stretching mode[12] of the Si–O bonds due to oxidation of Si in the film and silicon substrate. The spectrum of the Si-free *a*-C:H film shows the presence of C–H_n(*s*) stretching modes (2675–3250 cm^{-1}),[9–12] whereas the spectra of Si-containing *a*-C:H:Si films show the presence of not only C–H_n(*s*) stretching modes (2675–3250 cm^{-1}) but also Si–H_n(*s*) (2025–2250 cm^{-1}) modes.[9–11] The peaks in the 1240–1580 cm^{-1} range for all films were attributed to the mixing of Si–CH_3 wagging, C–H_n(*b*) bending, sp^3 C–C(*s*), and sp^2 C=C(*s*) modes.[9] The weak feature at 1700 cm^{-1} attributable to OH may be caused by surface contamination. The doublet peak (centered at ~2350 cm^{-1}) between Si–H_n and C–H_n peaks is associated with environmental CO_2. The intensities of the C–H_n(*s*) (2025–2250 cm^{-1}) and Si–H_n(*s*) (2675–3250 cm^{-1}) modes change markedly with the TMS flow rate as clearly shown in the inset of Fig. 3, whereas the intensities of all other peaks do not change significantly. The presence of Si–H_n bonds in the FTIR spectra suggests that Si dopants are coordinated with hydrogen atoms in the film structure.

The integrated intensities of the FTIR absorption peaks attributable to C–H_n(*s*) (2025–2250 cm^{-1}) and Si–H_n(*s*) (2675–3250 cm^{-1}) stretching vibrations, respectively, are calculated and plotted in Fig. 4(a) as a function of the TMS flow rate to elucidate the effect of Si incorporating on the chemical bonding. Figure 4(a) demonstrates that the integrated intensities of both C–H_n(*s*) and Si–H_n(*s*) modes increase with the increase of the TMS flow rate, which suggests the formation of a polymeric sp^3 C–H_n structure and

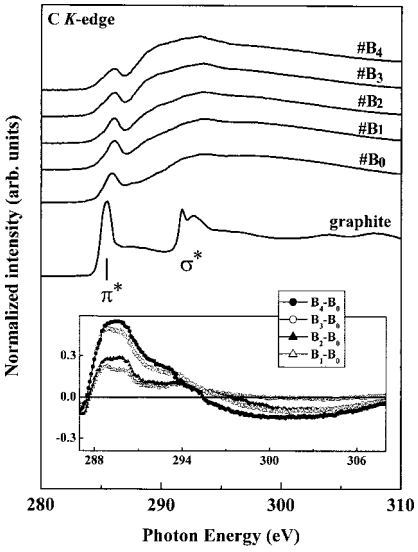

FIG. 1. Normalized C *K*-edge absorption spectra of the *a*-C:H:Si films, *a*-C:H film and the reference graphite film. The inset presents the difference curves between the spectra of the *a*-C:H:Si and *a*-C:H films.

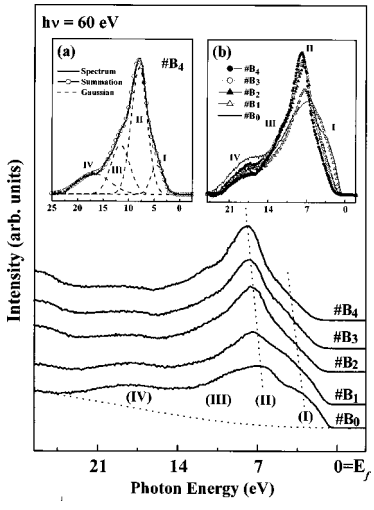

FIG. 2. Valence-band PES spectra of *a*-C:H:Si (at various TMS flow rates) and *a*-C:H. The inset (a) was obtained by deconvoluting the spectra of *a*-C:H:Si (B_4) with four Gaussian peaks. The inset (b) plots the spectra of all *a*-C:H:Si and *a*-C:H films after the base-line has been subtracted.

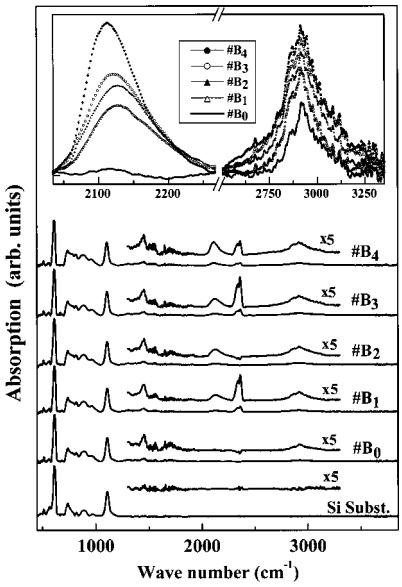

FIG. 3. Normalized FTIR spectra of films deposited with various TMS flow rates in the 400–3800 cm^{-1} range, in which the part in the 1200–3300 cm^{-1} range has been magnified five times for clarity. The inset shows the magnified $C-H_n(s)$ and $Si-H_n(s)$modes.

$Si-H_n$ bonding in *a*-C:H:Si films. Figure 4(b) compares Young's modulus (E) presented in Table I and the sp^2/sp^3 ratio obtained from C *K*-edge XANES (π^*/σ^*) and valence-band PES (π/σ) measurements to illustrate the effect of Si doping on *a*-C:H films. The sp^2 and sp^3-bonded carbon contents of each sample were estimated from the relative heights of the π^* (286.1±0.1 eV) and σ^* (293.0±0.1 eV) features (Fig. 1) and the π and σ features obtained by fitting to peaks **I** and **II** in the PES spectra [Fig. 2(b)], respectively. The sp^2/sp^3 ratio declines as the TMS flow rate increases and/or Si doping increases.

Figure 4(b) shows that the Young's modulus increases when the I_{sp2}/I_{sp3} ratio increases. This trend is in contrast to the usual observation that the increase of the Young's modulus is accompanied by a decrease of the I_{sp2}/I_{sp3} ratio in carbon-related materials, which concerns the exchange between graphite-like sp^2 bonding and diamond-like sp^3 C–C bonding. In the present case one needs to consider the effect of hydrogen and the increase in the number of $C-H_n$ and $Si-H_n$ bonds. The *a*-C:H:Si films normally contain dangling bonds saturated with hydrogen, which are relaxed so that the Young's modulus and the hardness decreases as the number of $C-H_n$ and $Si-H_n$ bonds increases. Figure 4(a) shows that in Si-containing *a*-C:H:Si films the number of $Si-H_n$ bonds increase with the TMS flow rate, i.e., the silicon content. Therefore, the incorporation of Si reduces Young's modulus and hardness. In other words, the increase of the number of $Si-H_n$ bonds relaxes the three-dimensional rigid network of *a*-C:H:Si films. The high hydrogen concentration in the TMS precursor used to deposit the film promotes the polymeric sp^3 $C-H_n$ bonding formation, which alters the bonding constraints of sp^3-bonded carbon and reduces the stress, hardness, and Young's modulus of the film.[13] Incorporating TMS also increases the numbers of $C-H_n$ and $Si-H_n$ bonds as mentioned earlier and bonds that are weaker than C–C bonds, so that the structural integrity of the films is weakened. [The bond energies of Si-H ($\leqslant$3.10 eV)[14] and C–H (3.51 eV)[14] smaller than C–C (3.70 eV).[15]] The formation of Si–C bonds (bond energy $\leqslant$3.10 eV)[15] in the interlayer between the film and substrate may also affect the hardness of the substrate. The increase of the density of voids, as noted by Baia *et al.* in hydrogen effusion experiments, with the increase of Si doping in *a*-C:H:Si films influences the connectivity and hardness of the network.[16]

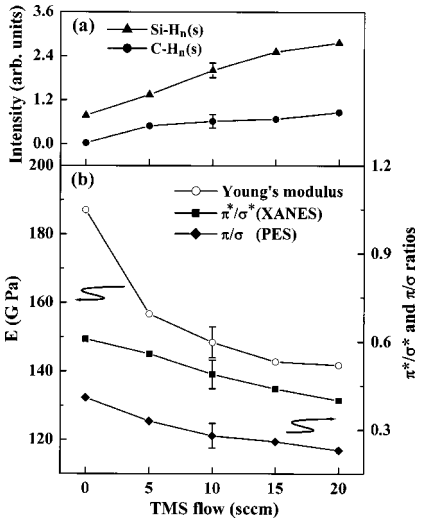

FIG. 4. (a) Integrated intensities of the $C-H_n(s)$ and $Si-H_n(s)$ modes obtained from FTIR spectra. (b) The π^*/σ^* ratio (from C *K*-edge XANES spectra), π/σ ratio (from valence-band PES spectra), and Young's modulus as functions of the TMS flow rate for all films.

This work was supported by the National Science Council of the ROC under Contract No. NSC 92-2112-M-032-025.

[1] P. R. Goglia, J. Berkowitz, J. Hoehn, A. Xidis, and L. Stover, Diamond Relat. Mater. **10**, 271 (2001).
[2] P. Papakonstantinou, J. F. Zhao, P. Lemoine, E. T. McAdams, and J. A. McLaughlin, Diamond Relat. Mater. **11**, 1074 (2002).
[3] J. Nithianandam, J. C. Rife, and H. Windischmann, Appl. Phys. Lett. **60**, 135 (1992).
[4] A. Hoffman, G. Comtet, L. Hellner, G. Dujardin, and M. Petravic, Appl. Phys. Lett. **73**, 1152 (1998).
[5] M. M. Gracía, I. Jiménez, O. Sánchez, C. Gómez-Aleixandre, and L. Vázquez, Phys. Rev. B **61**, 10383 (2000).
[6] H. M. Tsai, J. C. Jan, J. W. Chiou, W. F. Pong, M.-H. Tsai, Y. K. Chang, Y. Y. Chen, Y. W. Yang, L. J. Lai, J. J. Wu, C. T. Wu, K. H. Chen, and L. C. Chen, Appl. Phys. Lett. **79**, 2393 (2001).
[7] P. Reinke and P. Oelhafen, J. Appl. Phys. **81**, 2396 (1997); P. Reinke, P. Oelhafen, H. Feldermann, C. Ronning, and H. Hofsäss, J. Appl. Phys. **88**, 5597 (2000).
[8] S. Ghosh, P. Bhattacharya, and D. N. Bose, Appl. Phys. Lett. **68**, 2979 (1996).
[9] K. Mui, D. K. Basa, F. W. Smith, and R. Corderman, Phys. Rev. B **35**, 8089 (1987).
[10] R. A. C. M. M. van Swaaij, A. J. M. Berntsen, W. G. J. H. M. van Sark, H. Herremans, J. Bezemer, and W. F. van der Weg, J. Appl. Phys. **76**, 251 (1994).
[11] K. Chew, Rusli, S. F. Yoon, J. Ahn, V. Ligatchev, F. J. Teo, T. Osipowicz, and F. Watt, J. Appl. Phys. **92**, 2937 (2002).
[12] M. Ban and T. Hasegawa, Surf. Coat. Technol. **162**, 1 (2002).
[13] X. M. He, K. C. Walter, M. Natasi, S. T. Lee, and M. K. Fung, J. Vac. Sci. Technol. A **18**, 2143 (2000).
[14] K. R. Lee, M. G. Kim, S. J. Cho, K. Y. Eun, and T. Y. Seong, Thin Solid Films **308/309**, 263 (1997).
[15] C. S. Lee, K. R. Lee, K. Y. Eun, K. H. Yoon, and J. H. Han, Diamond Relat. Mater. **11**, 198 (2002).
[16] A. L. Baia Neto, R. A. Santos, F. L. Freire, Jr., S. S. Camargo, Jr., R. Carius, F. Finger, and W. Beyer, Thin Solid Films **293**, 206 (1997).